URSI-RCRS 2024, ARIES/GEHU, Bhimtal, India, 22 - 25 October, 2024

# Wide-Angle Beam Scanning Leaky-Wave Antenna Based on CRLH TL for Enhanced Radiation Performance in sub-6 GHz 5G

Sajeev K F [(1)], Nayana M D[(1)], Remya R[(1)], Gopikrishna M[(2)*]
(1) Dept. of Physics, Maharaja's College, Ernakulam, Kochi, Kerala, India, PIN 682011
(2) Dept. of Physics, Govt. Victoria College, Palakkad, Kerala, India, PIN 682301
*Corresponding Author Email – gopikrishna@gvc.ac.in

## Abstract

A novel leaky-wave antenna (LWA) utilizing substrate integrated waveguide (SIW) technology with beam scanning capabilities is presented in this paper. The antenna incorporates a Composite Right/Left-Handed (CRLH) Transmission Line (TL) and demonstrates beam steering from 29° (at 3.8 GHz) to -72° (at 6.7 GHz). It achieves a maximum gain of 12.5 dBi and exhibits high radiation efficiency, averaging 72% across its operating range. Full-wave simulations were performed using CST Microwave Studio.

## 1. Introduction

A leaky wave is a waveguide-based traveling wave that gradually loses energy through radiation into surrounding space. This intentional energy loss enables leaky wave antennas (LWAs) to achieve features like frequency beam scanning and wide operational bandwidth. LWAs are highly regarded for their ability to scan beams across frequencies and their broad bandwidth. The integration of substrate-integrated waveguide (SIW) has become common in LWA design, leveraging its resemblance to traditional waveguides [1]. Furthermore, combining CRLH TL meta-materials with SIW concepts creates a unique electromagnetic structure by arranging metallic vias in regularly spaced arrays on a planar substrate. This design mimics properties of conventional rectangular waveguides, enabling precise wave guiding and manipulation similar to standard waveguides. These structures excel in tasks such as beam steering and seamlessly integrate with planar circuits, making them ideal for high-performance antennas in modern communication systems and radar applications [3-7], collectively forming the CRLH LWA concept.

In this work, the unit cell comprises inter-digital stepped slots oriented at a 45-degree angle to the wave propagation direction (z-axis), optimizing radiation efficiency, especially in the broadside region. Each unit cell is interconnected by microstrip delay lines, facilitating effective beam steering. These periodically integrated delay lines enable precise control over signal phase and amplitude across the array, allowing for targeted beam steering in desired directions.

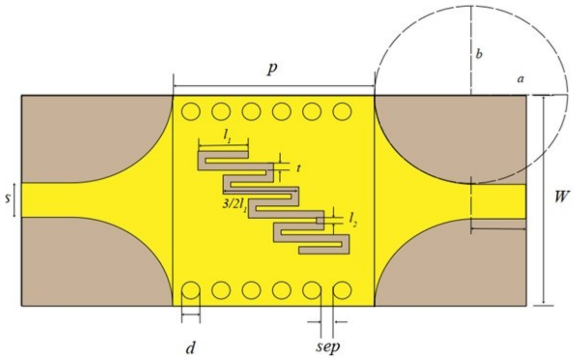


**Figure 1**. Unit-cell of the proposed LWA. $p$ = 20, $a$ = 10, $b$ = 10.2, $s$ = 3.6, $l_1$ = 5, $l_2$ = 0.75, $sep$ = 2.2 (All units in mm).

## 2. Design and Analysis: Unit Cell

The proposed CRLH SIW LWA, depicted in Figure 1 utilizes a unit cell with inter-digital stepped slots oriented at a 45° angle to the wave propagation direction (z axis). These slots serve a dual purpose: acting as series capacitors and functioning as the primary radiators, crucial for CRLH leaky-wave applications. This combination of series capacitor behavior and radiator role enables CRLH antennas to possess unique features like beam scanning capabilities and customized frequency responses.

The antenna is implemented using Rogers RO4003C substrate with specific parameters (dielectric constant $\varepsilon_r$=3.38, h = 1.57 mm and loss tangent $\delta$=0.001). The side walls are formed by strategically placing vias with a diameter of 0.8 mm, creating the SIW structure. The detailed parameters of the unit cell design can be found in Table 1. Figure 2 depicts the approximate equivalent electrical circuit of the antenna unit-cell. It consists of three parts, parts 1 and 3 are same as the equivalent circuit of a conventional SIW unit-cell [2] with distributed shunt capacitance $C_R$ and series inductance $L_R$, which gives the right-handed property. The 2$^{nd}$ part consists of the inter-digital capacitor $C_L$ and an inductance $L_L$ due to inter digital slots and vias respectively, that is LH contribution come through 2$^{nd}$ part and hence form the CRLH behavior.

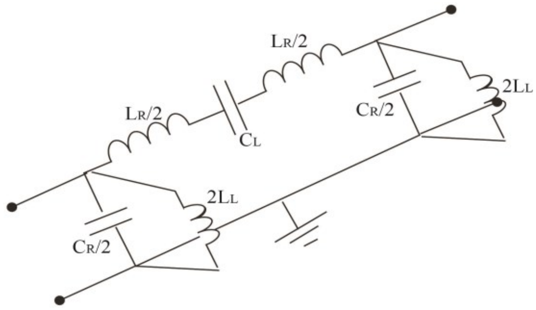


**Figure 2**. The equivalent electrical circuit of unit cell.

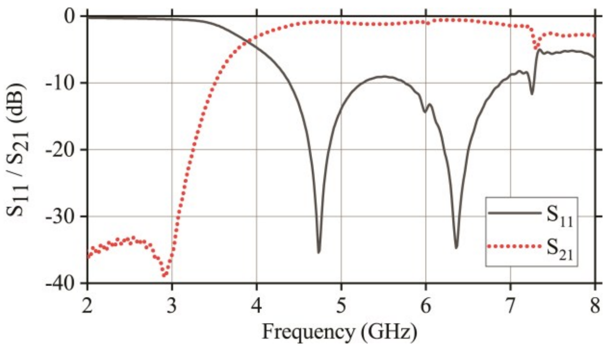


**Figure 3**. S-parameters of the CR/LH T-L Unit cell.

The simulated S-parameters are shown in Figure 3. It shows, the measured reflection coefficient is below -10 dB across the entire operating band. The dispersion (phase constant with frequency) and leakage (alpha with frequency) curves of the unit cell, which was created using the simulated scattering parameters, is shown in Figure 4. Equations (1) and (2) are used to plot this dispersion diagram using the simulated results of the scattering parameters [10-11] and it is plotted with normalized value of βp/π and αp/π. From the dispersion diagram, the balanced condition (zero phase constant) is found at 4.77 GHz and shows the airline ($k_0 = \omega\sqrt{(\mu_o \epsilon_o)}$) divides the curve into two regions: one is slow wave region (guiding wave region) which is above the airline and another is fast-wave region, it is the radiating region which is below the airline. Also, in the radiating region consist of two sections, one is LH section and other one is RH section in between broad side. In LH section, the radiating region corresponds to frequencies (4.2 GHz to 4.77 GHz) where the unit cell exhibits Left-Handed characteristics. In a Left-Handed material or structure, the phase velocity ($V_P$) and group velocity ($V_g$) of electromagnetic waves are in opposite directions. This often leads to unique properties such as negative refraction, backward wave propagation, and other unconventional wave behaviors. The RH region corresponds to frequencies (4.77 GHz to 5.7 GHz) where the unit cell exhibits Right-Handed characteristics. In a Right-Handed material or structure, the phase velocity and group velocity of electromagnetic waves are in the same direction, behaving more conventionally like materials found in nature. The presence of LH and RH sections in the radiating region indicates the complex electromagnetic behavior of the CRLH structure.

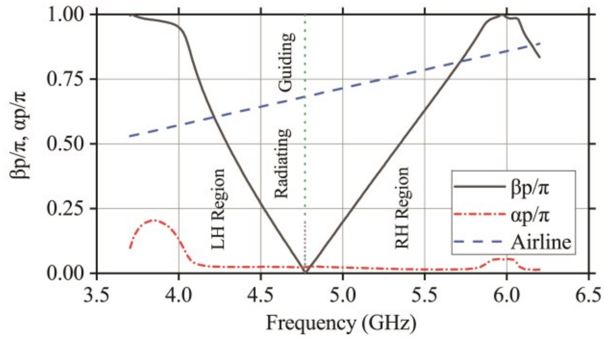


**Figure 4.** Dispersion diagram of the Unit cell.

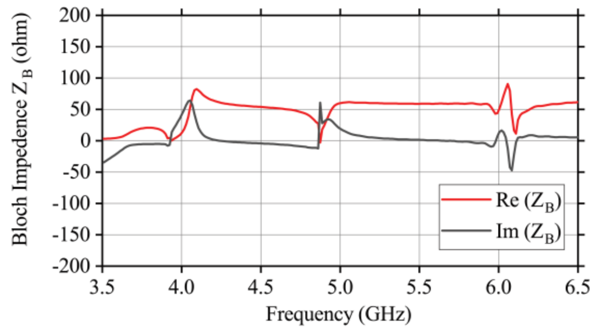


**Figure 5**. Bloch impedance versus frequency curve.

$$\beta = \mathrm{Im}\ (\cosh^{-1}(\frac{1-S_{11}S_{22}+S_{21}S_{12}}{2S_{21}})) \quad (1)$$

$$\alpha = \mathrm{R}\ (\cosh^{-1}(\frac{1-S_{11}S_{22}+S_{21}S_{12}}{2S_{21}})) \quad (2)$$

The radiation direction of the SIW LWA can be determined from the equation

$$\Theta_{rad} = \mathrm{Sin}^{-1}(\frac{\beta}{k_0}) \quad (3)$$

where $k_0$ is the wave-number of free spaces.

When $|\beta| < k_0$ , EM waves are fall into the category of fast waves and thus have the potential to be radiated from the LWA, otherwise the EM waves propagate as (guided) slow wave modes and cannot be radiated at all. The positive, zero, and negative value of the $\Theta_{rad}$ indicate forward, broadside, and backward radiation, respectively [8].

The concept of Bloch impedance is used to measure the impedance of a unit cell in a periodic transmission line. Bloch impedance can be computed using the unit cell's ABCD parameter or the s-parameter relation. It gives a point of reference for the periodic transmission structure's impedance matching. The Bloch impedance equation is expressed in Equation (4), and a graph of impedance versus frequency (Figure 5) is plotted to visualize its behavior.

$$Z_B = \pm Z_0 \sqrt{\frac{(1+S_{11})^2-(S_{21})^2}{(1-S_{11})^2-(S_{21})^2}} \quad (4)$$

The average of the real part of the Bloch impedance of the unit cell is approximately equal to 50 ohm and the

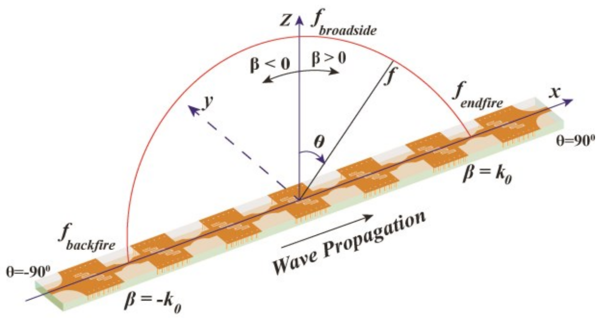


**Figure 6**. Proposed Leaky wave antenna.

imaginary part is very close to zero, providing a good matching, Hence, it nearly matches the transmission line's characteristic impedance, $Z_0$ [10],[12-13].

## 3. CRLH SIW Leaky-Wave Antenna

The proposed LWA has 7 identical unit cells and it is symmetrically arranged as shown in Figure 6. The three-layered structure of proposed antenna has a dimension of 290 x 22.5 $mm^2$. Each unit cell is connected by delay strips, which are optimized by simulation. The parameter values and dispersion relation for the unit cell have already been discussed in the above section. By optimizing this novel slot combination, ie, by arranging slots position and period of a unit cell and hence the matching between each unit cell is achieved. The unit cells are arranged in a linear manner and can be regarded as a periodic LWA.

Specifically, the periodicity permits the aperture field to be represented as the superposition of an infinite number of space harmonics, or Floquet waves, with phase constants

$$\beta_n = \beta_0 - \left(\frac{2n\pi}{p}\right),\ n=0, \pm1, \pm2,\ldots \quad (5)$$

where $\beta_0$ and $\beta_n$ are the phase constants of the fundamental harmonic and $n^{th}$ Floquet wave respectively. The issue of an open stop band (OSB) in periodic LWA can be addressed by incorporating the concept of CRLH transmission lines. To accomplish this, a balanced combination of series capacitors and shunt inductors must be used to create an effortless shift from the left- to the right-handed region.

When the series and shunt resonances of the CRLH transmission line are equal, it's considered to be in a balanced condition, which helps mitigate the OSB problem.

$$L_L C_R = L_R C_L \quad (6)$$

If the contributions from left-handed (LH) and right-handed (RH) components are equal (6) at a given frequency, it indicates a balanced condition in the system. In such a scenario, the propagation constant, which determines how waves propagate through a medium, can be determined by equation (7),

$$\beta = \beta_R + \beta_L = \omega\sqrt{L_R C_R} - \frac{1}{\omega\sqrt{L_L C_L}} \quad (7)$$

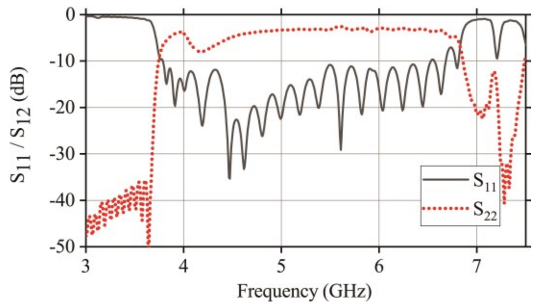


**Figure 7**. The simulated S-parameters of the antenna.

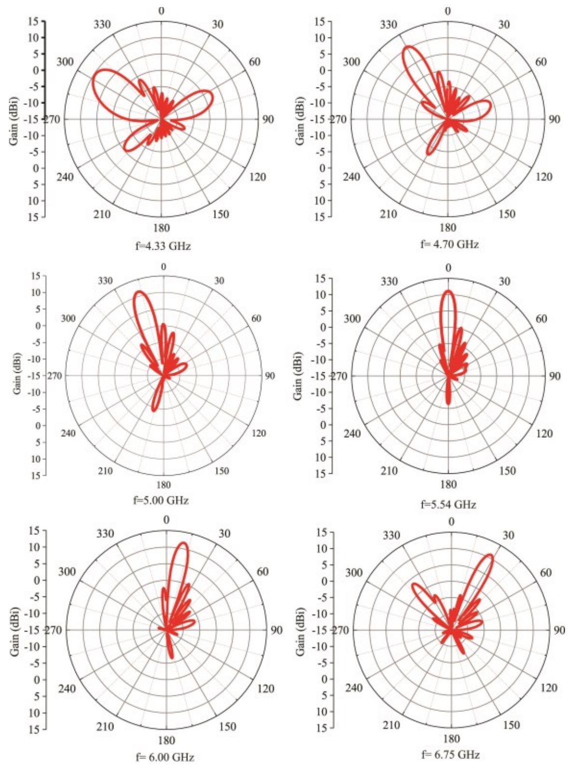


**Figure 8**. Radiation pattern showing beam-steering.

under balanced condition, $\beta$ =0, dispersion diagram of Figure4 indicates that an LH to RH transition occurs at frequency

$$\omega_0 = \frac{1}{\sqrt{L_L C_L}} \quad (8)$$

Figure 7 shows the simulated S-parameters of this antenna. The insertion loss is below -10dB, indicating good leakage radiation. The transmission curve ($S_{21}$) displays the leakage that happens in the array antenna and it measures the overall efficiency of the LWA. Also, the radiation is more effective in the LH region compared with the RH region. The measured $S_{11}$ is below -10 dB throughout the entire operating frequency band and it is observed that the operating band starts from 3.8GHz to 6.7GHz, with in this band the central frequency is at 5.4GHz (at broad side). The measured bandwidth in the proposed LWA is around 3GHz which is better than that of [9],[11] and [13].

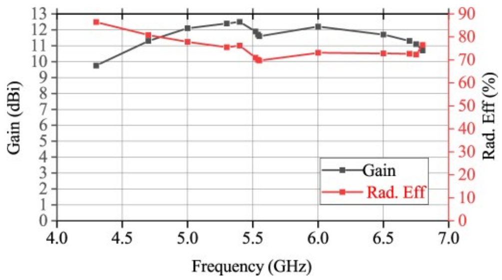


**Figure 9**. Gain and radiation efficiency versus frequency curve.

A consistent radiating beam observed, and it sweeps from $29^0$ (at 3.8GHz) to $-72^0$ (at 6.7GHz) is shown in Figure 8 and it shows both the forward and backward-radiation sweeping through broadside with different frequencies. Also, the side lob level (SLL) of the radiation is very low and it indicates that the energy or signal radiated in directions other than the main beam. This is particularly important in antenna design and radar systems, where low SLL helps in reducing interference and improving overall performance.

The gain and efficiency versus frequency are plotted in Figure 9 and it is observed that the antenna shows almost constant gain throughout its operating range (from 3.8 to 6.7GHz) and its maximum gain is 12.5 dBi. Antenna shows a good average of 72% radiation efficiency over the operating band, indicating excellent radiation performance.

## 4. Conclusion

This work introduces a novel substrate integrated waveguide (SIW) leaky wave antenna (LWA) designed and characterized for operation between 3.8 GHz and 6.7 GHz. The antenna's unit cell is based on CR/LH TL principles. It features a radiation pattern that varies from $29^0$ (at 3.8GHz) to $-72^0$ (at 6.7GHz) with frequency, showcasing pattern reconfigurability. With excellent gain and radiation efficiency, this antenna is well-suited for sub-6 GHz 5G systems.

## 5. Acknowledgements

The work presented in this paper is supported by the Science and Engineering Research Board (SERB), Department of Science and Technology (DST), India, under grant EEQ/2021/000931

## 6. References

1. Oliner, A. A., D. R. Jackson, and J. Volakis, “Leaky-wave antennas,” Antenna engineering handbook, Vol. 4, 12, 2007.
2. Mahmoud, S. F. and Y. M. Antar, “Leaky wave antennas: theory and design,” in 2013 30th National Radio Science Conference (NRSC), 1–8. IEEE, 2013.
3. Hirokawa, J. and M. Ando, “Single-layer feed waveguide consisting of posts for plane term wave excitation in parallel plates,” IEEE Transactions on Antennas and Propagation, Vol. 46, No. 5,625–630, 1998.
4. Hong, W., B. Liu, Y. Wang, Q. Lai, H. Tang, X. X. Yin, Y. D.Dong, Y. Zhang, and K. Wu, “Half mode substrate integrated waveguide: A new guided wave structure for microwave and millimeter wave application,” in 2006 Joint 31st International Conference on Infrared Millimeter Waves and 14th International Conference on Teraherz Electronics, 219–219. IEEE, 2006.
5. Deslandes, D. and K. Wu, “Integrated microstrip and rectangular waveguide in planar form,” IEEE microwave and wireless components letters, Vol. 11, No. 2, 68–70, 2001.
6. Huang, Y. and K.-L. Wu, “A broad-band ltcc integrated transition of laminated waveguide to air-filled waveguide for millimeter-wave applications,” IEEE transactions on microwave theory and techniques, Vol. 51, No. 5, 1613–1617, 2003.
7. Grigoropoulos, N., B. Sanz-Izquierdo, and P. R. Young, “Substrate integrated folded waveguides (sifw) and filters,” IEEE Microwave and wireless components letters, Vol. 15, No. 12, 829–831, 2005.
8. Jackson, D. R., C. Caloz, and T. Itoh, “Leaky-wave antennas,” Proceedings of the IEEE, Vol. 100, No. 7, 2194–2206, 2012.
9. Dong, Y. and T. Itoh, “Substrate integrated composite right-/lefthanded leaky-wave structure for polarization-flexible antenna application,” IEEE transactions on antennas and propagation, Vol. 60, No. 2, 760–771, 2011.
10. Sarkar, A., M. Adhikary, A. Sharma, A. Biswas, M. J. Akhtar, and Z. Hu, “Composite right/left-handed based compact and high gain leaky-wave antenna using complementary spiral resonator on hmsiw for ku band applications,” IET Microwaves, Antennas & Propagation, Vol. 12, No. 8, 1310–1315, 2018.
11. Sabahi, M. M., A. A. Heidari, and M. Movahhedi, “A compact crlh circularly polarized leaky-wave antenna based on substrate integrated waveguide,” IEEE Transactions on Antennas and Propagation, Vol. 66, No. 9, 4407–4414, 2018.
12. Otto, S., A. Rennings, K. Solbach, and C. Caloz, “Transmission line modeling and asymptotic formulas for periodic leaky-wave antennas scanning through broadside,” IEEE transactions on antennas and propagation, Vol. 59, No. 10, 3695–3709, 2011.
13. Yang, Q., X. Zhao, and Y. Zhang, “Composite right/left-handed ridge substrate integrated waveguide slot array antennas,” IEEE Transactions on Antennas and Propagation, Vol. 62, No. 4, 2311–2316, 2014.